Stand-alone Photovoltaic System using an UPS Inverter and a Microcontrolled Battery Charger based on a Boost Converter with a 3 State-Commutation Cell.

Samuel V. Araújo, René P. Torrico-Bascopé, Fernando L. M. Antunes, Edílson Mineiro Sá
Electrical Engineering Department
Federal University of Ceará
Campus do Pici s/n, Caixa Postal 6001.
Fortaleza, CE 60.455-76, Brazil
sva82@terra.com.br , rene@dee.ufc.br, fantunes@dee.ufc.br, edilson@dee.ufc.br

Abstract – This paper presents a stand-alone photovoltaic energy system aimed for small power consumer applications in isolated areas of the countryside of Brazil. In order to develop a cost-effective and simple product, a double power conversion UPS (Uninterruptible Power Supply) was analyzed and modified. A whole new battery charger was implemented using a PIC microcontroller equipped with a MPP seeking algorithm, to maximize the energy extracted from the solar panels, and a supervisory unit to control the charge process of the batteries, in order to ensure that they are fully charged.

I. INTRODUCTION

Despite the great abundance of solar potential in the Northeast of Brazil, that in some cases surpasses 4,900 Wh/m^2 per day, it is the access to electricity still a critical problem, especially in the countryside. In the year 2000, approximately 14.2% of those rural houses did not have a stable supply of electrical energy.

Trying to solve this problem, an electrification program was launched by local and federal governments with the purpose to expand the access to electric energy within the state either by the expansion of the grid or by the installation of electric generators based on renewable energy sources. The investments, in a range of U$ 50.00 millions dollars have been done.

In order to provide a non-expensive, robust and easily implementable system, a partnership between a local power supply manufcturer and a university laboratory was established.

The primary objective was to obtain a stand alone electricity generator system supplied by solar photovoltaic energy using a commercial 1 kVA Double Power Conversion UPS. UPS in this level of power are very popolar in the Brazilian market, where SOHO-consumers (small offices, home offices) protect their individual computers from energy outages.

II. DESCRIPTION OF THE PROPOSED BATTERY CHARGER TOPOLOGY

Basically, all non-isolated DC-DC converters are made of 3 components: an input voltage source, the load output with a capacitor connected in parallel and the converter cell, with 3 input terminals whose type of connections will determine the converter topology.

The commutation cell firstly proposed in [1] and used in this work is obtained from a classic current fed push-pull converter.

The first step to obtain this cell consists on referring the secondary side of the transformer to the primary side, forming an autotransformer with symmetrical turns as shown in Fig. 1 (b).

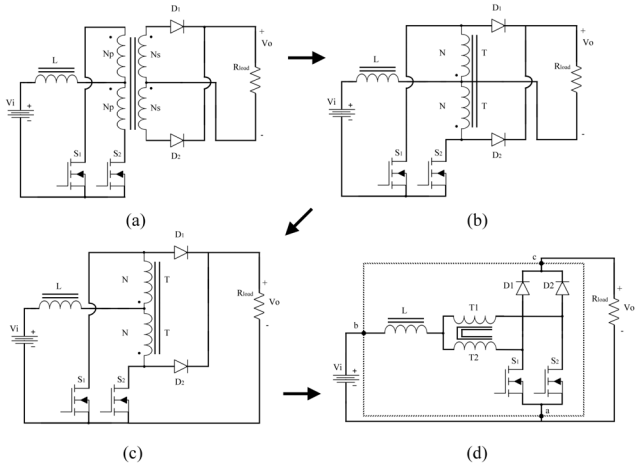

Fig. 1. Obtaining a 3-state commutation cell.

The negative output terminal that was previously connected to the central tap of the transformer is now connected to the negative input terminal as shown in Fig. 1 (c). Rearranging the circuit, the representation on Fig. 1 (d) is obtained.

In order to get a boost converter with this commutation cell, the 3 points are connected as shown in Fig. 2.

When the duty cycle of this converter is limited within the range of 0% to 50%, the boost converter operates on the non-overlapping region, meaning that the two MOSFETs won't conduct at the same time. Since the relationship between the nominal voltages of the photovoltaic array and of the batteries was always below 0.5, only this mode was used for this project.

The operation of the converter on the continuous conduction mode and on the non-overlapping region can therefore be divided on 4 stages.

On first stage, as illustrated in Fig. 2, S1 is turned on and S2 off. This leads to the blockage of D1, while D2 continues forward biased. The current from the source is equally divided between T1 and T2 (since both windings of the autotransformer have the same number of turns) and grows linearly, charging the input inductor.

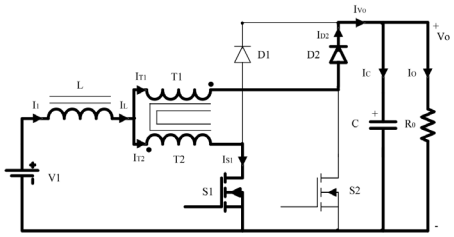

Fig. 2. 1st operational stage.

Fig. 3 illustrates the second stage, when S1 is blocked. The voltage across the inductor is inverted in order to maintain the magnetic flux across the core. Therefore, D1 is now forward biased, while D2 continues to conduct. The energy stored on the inductor is now sent to the load and because of the complementary polarity of the currents over each side of the autotransformer, the magnetic flux on it is null.

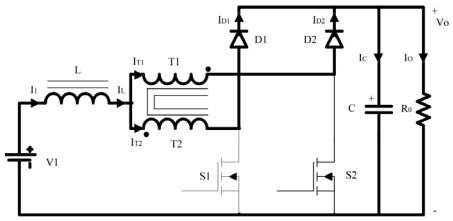

Fig.3. 2nd and 4th operational stages.

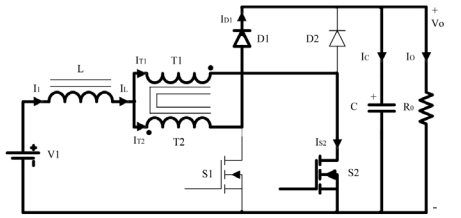

Fig.4. 3rd operational stage.

The third stage, as shown in Fig. 4, is symmetrical to the first one, with the change that now S1 and D2 are blocked while S1 is turned on and D1 continues to conduct. The fourth stage is equal to the second one.

The static gain is defined as the relationship between the output and input voltages and is calculated with the average voltage over the inductor. Its relation is the same as the one of the classical boost topology.

In the discontinuous mode of operation, the current across the input inductor goes to zero before reaching the end of the commutation cycle. It is no advisable to work on this region because of its non-linearity that makes it difficult to implement the control circuit. When compared to the classical boost topology, this new converter has the advantage of having a larger continuous conduction operation area. This leads to a reduction of the input inductance to half of its previous value.

A. Theoretical waveforms

The main waveforms in the non-overlapping operation, with continuous conduction are presented on the Fig. 5. It is important to notice that the input current is non-pulsated as well as the output current, that has 2 levels. Besides, the frequency of the currents is the double of the switching frequency of the MOSFETs, allowing the reduction of weight and volume of reactive elements.

In the presented situation, 50% of the input power is directly transmitted to the load through the diodes, so that the amount of power processed and lost on the MOSFETs by conduction and switching losses could be reduced, enhancing the converter's efficiency.

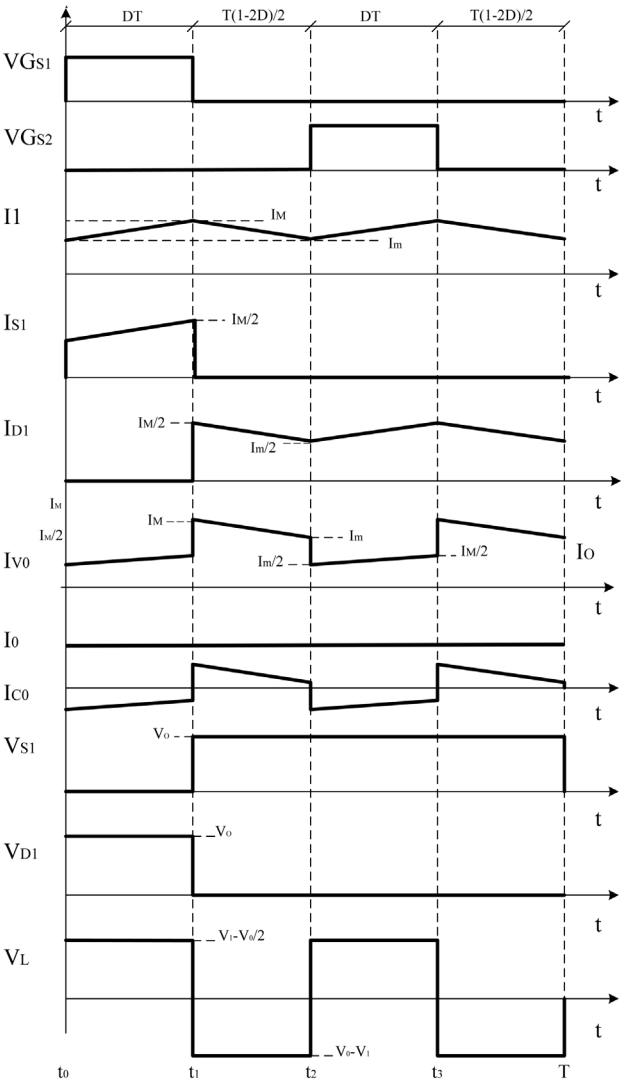

Fig. 5. Theoretical waveforms.

III. CONTROL STRATEGY OF THE BATTERY CHARGER

The PIC16F877 microcontroller was chosen to operate the control circuit due to its processing speed, 10 bit A/D converter and flexible programming options that allowed several tests using different algorithms.

A. Maximum power point tracking

The control circuit performs basically two operations. The

first one is to search for the maximum power point and keep the converter operating around it, the so-called MPPT. The chosen algorithm to perform this task was the Perturb and Observe that, by modifying the converter's duty cycle, promotes the perturbation that will lead to a change on the amount of power extracted from the photovoltaic array. If this amount is greater than the one processed on the previous control cycle, the next perturbation will be done on the same direction.

Since batteries are connected to the output, the voltage on this side can be considered as constant for small intervals of time [2]. This way, measuring just the current that is flowing into the batteries is enough to have an estimation of the power processed at the output, which leads to a simplification of the MPPT algorithm and a reduction on the amount of sensors.

These current measurements are done by using a Hall-Effect current sensor which avoids the power dissipation of a shunt resistor and provides electric insulation, protecting the control circuit. The resultant MPPT algorithm is illustrated in Fig. 6.

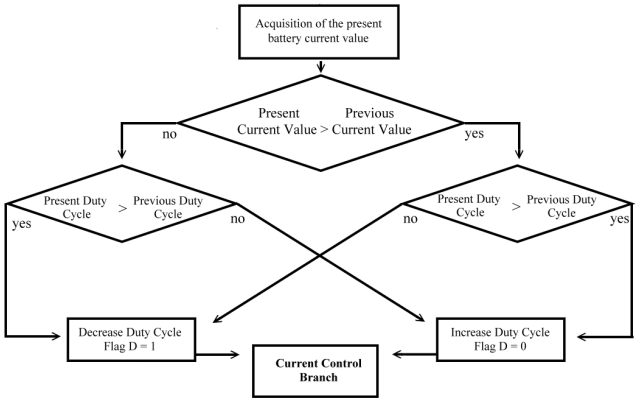

Fig. 6. MPPT algorithm schema.

In order to test the efficacy of this algorithm, a "sweeping mode" was developed. It operates by continuously changing the converter's duty cycle, making it work on all possible operational points. This mode can be seen on the first part of the curve in Fig. 7 that displays the amount of power extracted from the photovoltaic array.

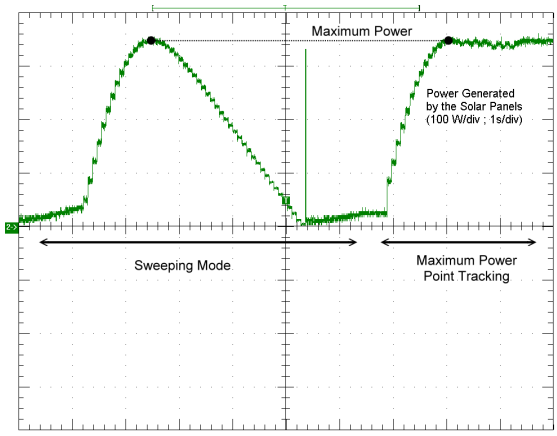

Fig. 7. Testing the efficacy of the MPPT (100W/div; 1s/div).

At a certain moment, the "sweeping mode" was disabled and the MPPT was enabled. It was then possible to observe that in approximately 1 second the control reached the maximum power point, ensuring the efficacy of the algorithm. It is important to notice that this test was made under constant solar radiation levels, ensured by the use of a pyranometer.

B. Batteries charging control

Due to the intermittent dynamic from off-grid photovoltaic systems, the batteries are generally considered as one of its most critical components. If inappropriate charge and discharge methods are used, the lifetime of the batteries is greatly reduced, implying on further expenses for the system.

Therefore, it is important to maintain the batteries at the highest possible State of Charge (SOC), which means, how much power (generally measured as a percentage of nominal capacity of the battery) is still available from it.

According to [3], a 100% SOC is guaranteed when the batteries reach a voltage of 2.4 V/cell when charged with a current of C/100. For example, a 12V 150 Ah battery will be fully charged when it reaches a voltage of 14.4V under a charging current of 1.5 A.

Using this concept, an interesting algorithm is proposed in [4]. Initially the system operates with a MPPT. When a desired level of voltage is reached, a current regulation algorithm is initialized.

This current regulation is done by setting the maximum current as a system variable and using the duty cycle modifications of a buck converter as control parameters, that is, duty cycle increments result in photovoltaic array voltage reduction and vice versa. The current is reduced in successive steps as it reaches the higher battery voltage level until the minimal value of C/100 is obtained.

The charging algorithm here proposed implements a slightly different approach since the current limitation is done by adding a branch (shown in Fig. 8) to the already proposed Perturb and Observe algorithm.

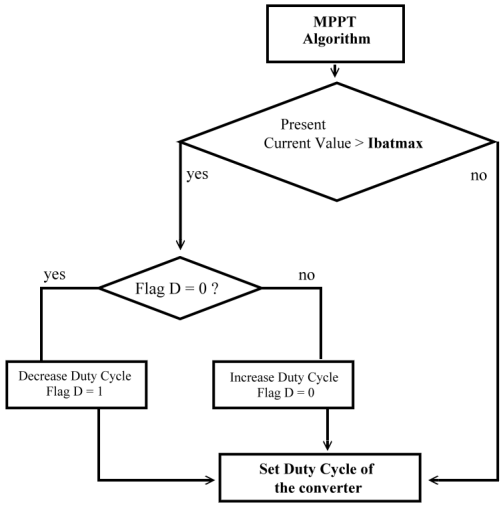

Fig. 8. Current control branch.

By remembering that the objective of the MPPT here implemented is to increase the current sent to the batteries; a simple way to provide current control is by inverting the present decision of the MPPT algorithm block whenever it is necessary to reduce the charging current.

Therefore, the additional current control branch verifies if the present value of the current surpasses the one determined by the system variable "Ibatmax". If this happens, the decision of increasing or decreasing the duty cycle set by the MPPT on the present control cycle is inverted and the system flag "D" is changed in order to inform the control about the direction of the perturbation.

The task of setting the value of the variable "Ibatmax" is done by the charge control algorithm, shown in Fig. 9.

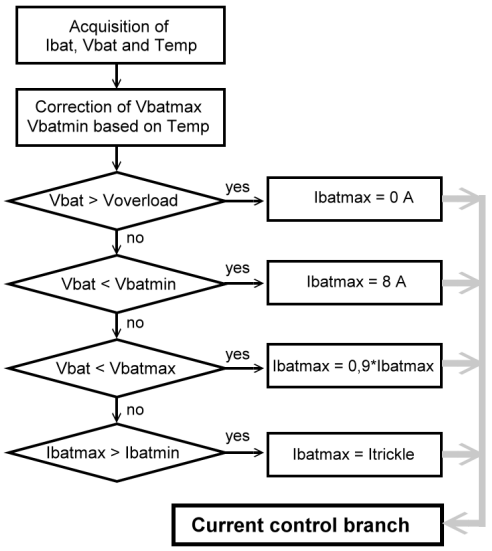

Fig. 9. Charge control algorithm.

Initially the values of the batteries present voltage (Vbat), charging current (Ibat) and temperature (Temp) are acquired. The temperature value is used to correct the voltage set-points $V_{overload}$ (voltage level near overcharge of the batteries), $Vbat_{max}$ (voltage level characterized by the condition of 2.4V/cell) and $Vbat_{min}$ (level of voltage where the batteries are considered as discharged, approximately 2.12V/cell). This correction is important since these values are greatly influenced by the temperature of the batteries.

The next control step is used for safety reasons and avoids overvoltages on the batteries that may damage them. In this case, variable "Ibatmax" is set to zero and the converter will be turned off, making the current from the array zero. For the battery bank used in this system, Voverload was set to 60.0 V.

The next step tests if the batteries reached the voltage level named as $Vbat_{min}$ (50.8 V), as it may happen if the load requires any energy of the batteries. Consequently, the voltage was reduced and when this level is reached, the value of Ibatmax will be set to the maximum possible value, in order to ensure that all the possible power needed by the system is fed by the photovoltaic array capacity, if available.

If the voltage of the batteries is higher than $Vbat_{min}$, it is checked if the batteries reached a voltage superior to $Vbat_{max}$, which is defined according to the condition of 2.4V/cell and results in a value of 57.6 V for the battery bank used on this project. If not, further charge of the batteries must be made. In case of affirmative, the charging current must be reduced to a lower level.

The next condition checks if it is possible to reduce the value of Ibatmax, by comparing it with a predetermined value named as Ibatmin that corresponds to C/100. If the minimal current is reached, the charge process is finished and it is guarantied that a 100% SOC was reached. Then, the current is set to a small constant value in order to avoid self-discharge and feed necessary circuitry consumptions.

As advantages of this approach, the converter is operating, whenever it is possible, on the Maximum Power Point, enhancing the use of the array available power and providing always the maximal allowable current value, optimizing the whole charge process.

IV. INVERTER ANALYSIS

Unlike in other countries, UPS systems have in Brazil a considerable market share focused on home and small office users. Theses small systems, in the range from 700 VA to 2000 VA, have normally an autonomy of 10 minutes when feeding full load.

By using parts of an already commercial power system, it will be therefore possible to achieve a final product in a faster way, reducing production costs and enabling a fast answer to the demands of the market.

Since it was aimed in the project the construction of a 1kVA photovoltaic system, an UPS system within this same capacity was chosen. Besides, knowing that in a stand-alone photovoltaic systems the inverter will be most likely functioning almost all the day, the system equipped with the Double Power Conversion topology, shown in Fig. 10, was the most suitable for this kind of application.

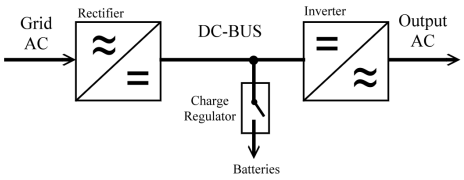

Fig.10. Double power conversion topology.

The voltage available from the net is rectified and transmitted to a DC bus where the batteries are connected. An inverter is then responsible for generating a regulated AC sinusoidal voltage. Among the advantages of this topology, it can be said that now the load is totally protected against problems and imperfections of the net like, for example, power sags, power surges, brownouts, line noise, frequency variations, switching transients and presence of harmonics. Since the inverter is always feeding the load, transient problems during the operation of bypasses (normally common in the Standby topology) are also eliminated. As disadvantages, this kind of system tends to show lower efficiency levels since it is always processing all of the consumption of the load. The used UPS also provided

protection against overloading, short-circuit and batteries deep dischargers.

V. INVERTER MODIFICATIONS

The modifications on the UPS followed two main directions. Since low levels of efficiency are unacceptable for photovoltaic systems due to the high cost of this kind of energy, changes were done on the step-up output transformer in order to reduce magnetizing currents, harmonics through the windings and non-linear magnetic flux phenomena (especially caused by constructive methods). Other suggestions like changing the material of the transformer core and using power switches with lower conduction and commutation losses were also discussed and are at the moment being analyzed by the manufacturer.

The second modification was simply deactivating the battery charger that already existed on the UPS and substituting it with the new developed converter. The feature of protecting the batteries against deep discharges was, nevertheless, still active at the inverter's circuit.

VI. EXPERIMENTAL RESULTS

A prototype was built, according to the requirements of the project, as follows:

Po = 588 W Output power
Fs = 20 kHz Switching frequency
VI = 33.6 V Input voltage at MPP
V0 = 48 V Output nominal voltage of batteries

The following waveforms were taken with operation near the nominal region, with the converter fed by a controllable DC Power Source and using resistances as load. They were not taken using the photovoltaic array and batteries since their behavior is too instable and would compromise the comparison between the waveforms.

Fig. 11 presents the current and voltage waveforms of the input inductor. It is possible to observe that the frequency is the double of the switching frequency.

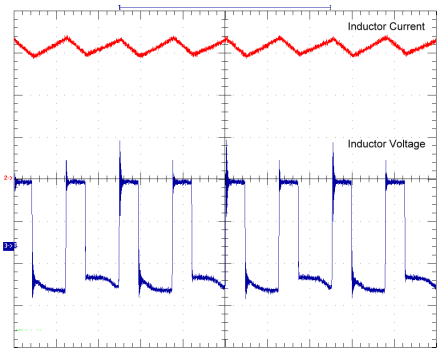

Fig. 11. Inductor Current (5 A/div) and Voltage (10V/div;20us/div).

When switch S1 is turned on, the voltage across the T1 winding of the autotransformer reaches theoretically the negative value of the input voltage, as can be seen on Fig. 12, leading to the blockage of the diode D1.

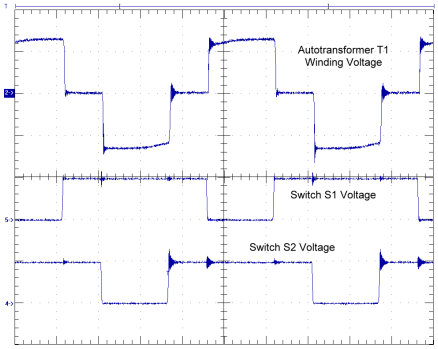

Fig. 12. Voltage across the autotransformer T1 winding (20V/div), Switch S2 (50V/div) and S1 (50V/div; 10us/div).

As the switch on the other commutation-cell is turned on, a positive voltage component is reflected since both windings have complementary polarities, providing current balance.

Fig. 13 presents the voltage and current waveforms of the switch S1. The blocking voltage overshoot is justified by parasitic inductances present at the wire of the jumper used for current measuring, since on the other switch these overshoots were not present. Small oscillations on the voltage were caused by some temporary discontinuities on the control signal originated by speed differences of the used logic gates and flip-flop, since 2 switching signals working from 0 until 100% with superposition and a delay of 180° were necessary. This problem can be solved by employing LS logic circuits instead of HC, since these are much faster than the first ones.

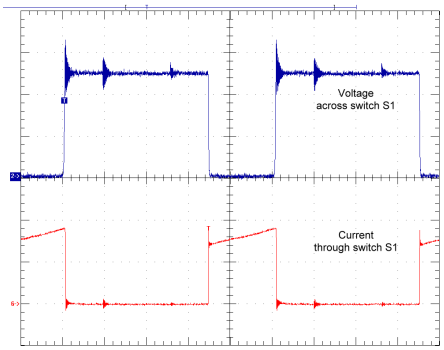

Fig. 13. Voltage (20V/div) and Current (5A/div; 10us/div) on switch S1.

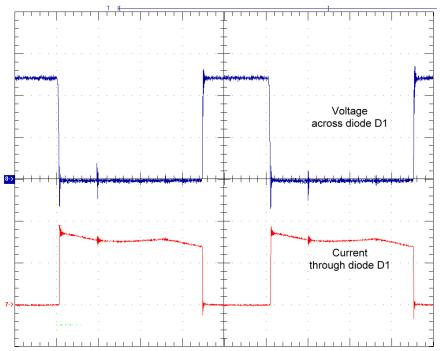

Fig. 14. Voltage (20V/div) and Current (5A/div; 10us/div) on diode D1.

In Fig. 14 are illustrated the voltage and current waveforms of the diode D1, where is possible to observe the complementarities with the ones from S1, since the diode is forward biased only when the correspondent switch is turned off.

The battery charger efficiency was then measured for three different input voltage levels, as shown in Fig. 15. The value of the load resistance was changed in order to vary the processed power, with the care of maintaining the input and output voltage constant, by means of respectively controlling the DC power source and slightly modifying the converter's duty cycle.

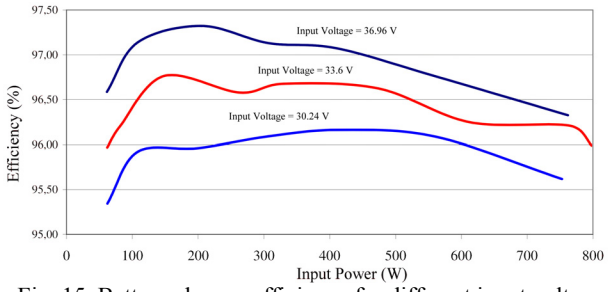

Fig. 15. Battery charger efficiency for different input voltages.

Fig. 16 illustrates the charge operation of the system during approximately 8 hours and is divided into 3 regions. The first one indicates that the variable "Ibatmax" is still on the maximum value and therefore there is no current regulation.

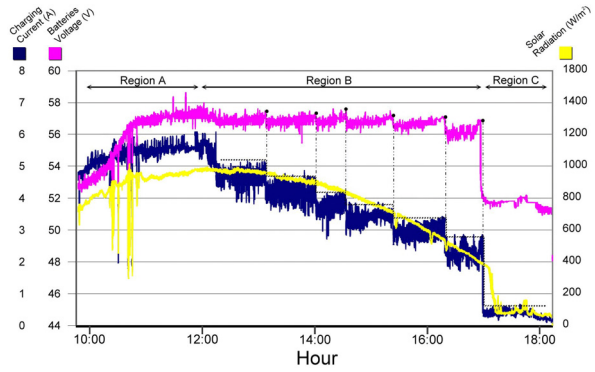

Fig. 16. System's operation for 8 hours illustrating control steps.

The interval B shows the successive current regulation steps. When the last reduction cycle is finished, a trickle current (interval C) is admitted and as a consequence the batteries voltage is reduced to a lower level.

A photo of the assembled prototype can be seen in Fig. 17, with the whole system using the original case of the UPS.

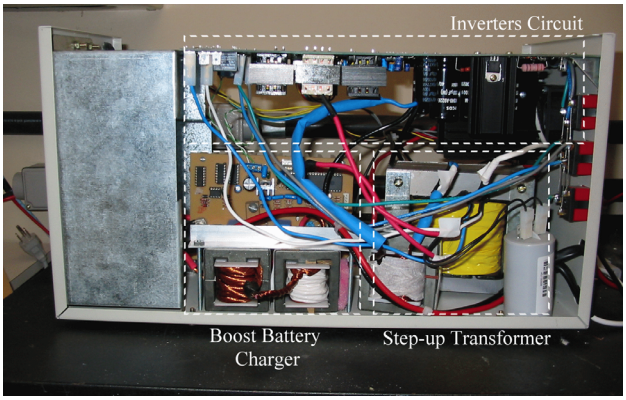

Fig. 17. Assembled Prototype

VII. CONCLUSIONS

This paper has presented the development of a stand-alone photovoltaic-based energy production system to be used in isolated places in the countryside of Brazil away of the grid.

By using an already commercially available inverter, developed by a local manufacturer, it was possible to propose a robust and non-expensive system,.

The battery charger here proposed reached high levels of efficiency that could be enhanced by design optimization.

Special algorithms developed lead to the operation of the PV panel at the MPP, and also control the the charge process of the battery bank provided a joint solution between maximum use of the photovoltaic array and safe maintenance of the batteries at the highest SOC, enhancing the reliability and lifetime of the whole system.

In full load the global efficiency of the system is around 85%. To improve such value, optimization in the inverter stage must be realized.

VII. ACKNOWLEDGMENT

The authors would like to thank Brazilian Research and Project Financing agencies – FINEP and CNPq for the financial support of this research.

VII. REFERENCES

[1] G. T. Bascopé, Barbi, I.; Generation of a family of non-isolated DC-DC PWM converters using new three-state switching cells, IEEE Power Electronics Specialists Conference 2000, vol. 2, 18-23 June 2000.

[2] D. Shmilovitz, On the Control of Photovolic aximum Power Point Tracker via Output Parameters, IEE Porc. Electr. Power Appl., Vol 152, No. 2, March 2005.

[3] D. Linden, Handbook of Batteries, Mc.Graw Hill, 2nd. Edition, 1995.

[4] E. Koutrolis, K. Kalaitzakis, "Novel battery charging regulation system for photovoltaic applications", in IEEE Proc.-Electr. Power Appl., vol 151, No. 2, March 2004.